IN-VENTO 2026
International Conference of the Italian Association for Wind Engineering
Bari, September 13th – 16th, 2026

Are long-span bridges sensitive to tornado-induced flutter-like vibration? An exploratory study

Luca Caracoglia[a]

[a]*Northeastern University, Boston, Massachusetts 02115, USA, l.caracoglia@northeastern.edu*

SUMMARY:
This study examines the research question whether bridge flutter instability can be triggered by repeated tornado strike. Based on recent results using the Floquet Theory to formulate the bridge flutter problem under non-stationary thunderstorm winds (Caracoglia, 2025), a new state-space model is proposed herein, which describes the "mean" tornado field by transient outflows that are repeated periodically with a given strike periodicity. This flow feature imitates the touchdowns of repeated tornadoes in the proximity of the deck, traveling towards the structure with a trajectory orthogonal to the deck's longitudinal axis. In this preliminary study, the mean tornado flow replicates the tangential wind speed of the tornado at the deck height but neglects the vertical velocity inflow. The tornado wind field accounts for the tornado core spatial dimensions, i.e., the primary vortex radius compared to the deck span length, and the temporal variations in the mean-wind flow velocity. Although these assumptions are simplified, the study demonstrates that the critical flutter velocity can be finite. Specifically, the model is used to quantify the maximum tornado tangential velocity, which causes diverging deck vibration. The Messina Strait Bridge (1992 design) is used to illustrate the model by preliminary results.

Keywords: Long-span bridges, aeroelasticity, flutter, non-stationary tornado winds

1. INTRODUCTION

The issue of tornado strike on long-span bridges has received much attention in the last years due to an increasing number of tornadoes causing damages to structures or infrastructures. Most existing studies have focused on the simulation of the tornado wind field and pressure loads at representative cross sections of an elevated bridge deck by computational fluid dynamics (e.g., Cao et al., 2019). The main research question has consequently been about the susceptibility to large-amplitude buffeting vibration. This study addresses the question about the susceptibility of a long-span bridge deck to a catastrophic, diverging vibration regimes, termed as "flutter-like". Flutter is the coupled bending-torsion aeroelastic instability of the deck that usually concerns the bridge designer [e.g., Jones and Scanlan (2001)].

Caracoglia (2025) explored the use of the Floquet Theory to formulate the bridge flutter problem under non-stationary thunderstorm winds. The same approach is employed in this work to construct a state-space model that describes the "mean" tornado wind field of a sigle-cell tornado as a sequence of transient outflow events that repeatedly impact the bridge deck. The outflow imitates the touchdowns of a sequence of tornadoes with a given "strike" periodicity, traveling towards the deck superstructure with a trajectory orthogonal to the bridge deck's longitudinal axis. The objective of the work is to verify whether the tornado-induced flutter velocity can be finite. The Messina Strait Bridge model (1992 design) illustrates the model.

2. BACKGROUND

2.1. Tornado Wind Field and Deck Load Model

The tornado flow field of a single-cell tornado replicates a slowly-varying mean wind velocity field, as it approaches the deck superstructure given an initial touchdown point of the tornado center with initial coordinates (X_0, Y_0) (Fig. 1). The touchdown is located at an offset coordinate

Y_0 with respect to the deck plan view (with central span length $\ell_{\mathtt{cs}}$ and width B). The tornado center travels with horizontal translational velocity $U_{\mathtt{trans}}$ towards the deck in Fig. 1, with arrival time $t_1 = |Y_0|/U_{\mathtt{trans}}$ from touchdown; $X_0 > 0$ also defines the point of impact of the storm with the deck. The main component of the outflow is represented by the tangential wind speed $V(r,t)$, which depends on both time t and radial relative horizontal distance between the tornado center and the deck cross-section (sectional coordinate x in Fig. 1).

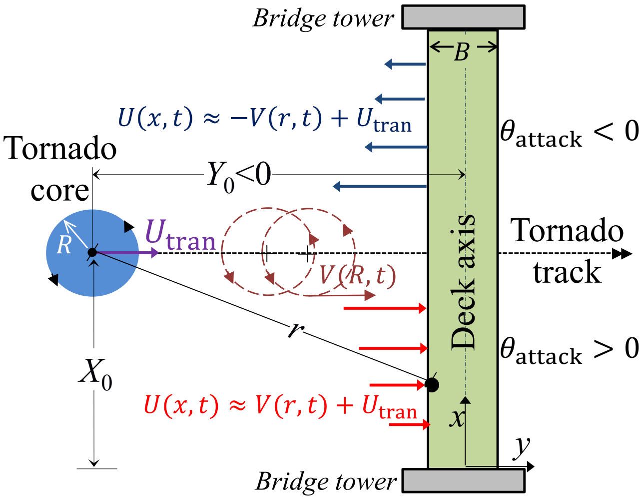

Figure 1. Schematic plan view of the tornado wind field model and coordinate system at deck height

The mean tornado wind field is simulated by Fujita tornado model (Fujita, 1978), composed of an inner core (whose reference distance from the tornado center is designated by r_n - not shown) and the outer core, where maximum tangential and radial velocities occur and whose reference distance from the tornado center is designated by the parameter R (Fig. 1). The "core" radius is $0 < R \ll \ell_{\mathtt{cs}}$. Fig. 1 demonstrates that the tornado is a local excitation phenomenon when considering a line-like horizontal structure. The wind velocity component orthogonal to the bridge deck, used in the aeroelastic analysis as the reference to compute the sectional wind loads, is $U(x,t) \approx U_{\mathtt{trans}} \pm V(r,t)$ by vector summation of the translational and tangential velocity components. Because of the tornadic tangential circulation, $V(r,t)$ switches sign at $x = X_0$ (from positive for $0 \leq x < X_0$, to negative for $X_0 < x \leq \ell_{\mathtt{cs}}$). For example, the magnitude of $U(x,t)$ is largest at $x = (X_0 - R_c)$. Fig. 1 also displays the variable intensity of $U(x,t)$.

The $U(x,t)$ wind field model does not account for the vertical tornadic velocity component, as a first approximation, also noting that, in the Fujita model, this term only exists in the circumferential region between r_n and R. Furthermore, the horizontal, radial inflow speed component is usually negligible at the deck height, which is usually above the "inflow layer" height H_i (Fujita, 1978), given the values of r_n and R. Thus, the tangential velocity $|V(r,t)| \gg U_{\mathtt{trans}}$ primary depends on the separation distance in x direction (Fig. 1), i.e., $r \approx |x - X_0|$ as

$$U(x,t) = U_{\mathtt{trans}} + V_{\mathtt{max}} \Psi_{\mathtt{pts}}(t) F_{\mathtt{fj}}(x) \mathrm{sgn}(X_0 - x). \tag{1}$$

Eq. (1) separates the two features of the wind field as two intensity functions (temporal modulation $\Psi_{\mathtt{pts}}(t)$ and spatial intensification $F_{\mathtt{fj}}(x)$), which are found from the tornado wind field model (Fujita, 1978); $V_{\mathtt{max}}$ denotes the maximum tangential velocity of the tornado at deck height and $\mathrm{sgn}(\cdot)$ is the "signum" function. Finally, the aeroelastic load is simulated by considering the standard load formulation in time domain, i.e., by indicial function approach (Scanlan et al., 1974), in which the aeroelastic properties of the deck are approximated by the stationary-wind unsteady load functions in the absence of specific experimental data (Caracoglia, 2025). The dependence on the tornado wind field is imposed by setting the kinetic pressure proportional to $U^2(x,t)$, derived from Eq. (1) as

$$U^2(x,t) = V_{\mathtt{max}}^2 \Psi_{\mathtt{pts}}^2(t) \mathscr{I}^{(2)}(x). \tag{2}$$

Fig. 2 illustrates the mean-square (MS) temporal modulation $\Psi_{\mathtt{pts}}^2$ *vs.* dimensionless time $\tau = t\omega_k$, with ω_k angular frequency of the first deck torsional mode "k" and MS spatial intensification $\mathscr{I}^{(2)} > 0$ *vs.* longitudinal deck coordinate $0 \leq x \leq \ell_{\mathtt{cs}}$. The panels replicate the features of a sequence of repeated "Fujita tornadoes" of core radius $R = 200\,\mathrm{m}$, with "periodic tornado strike" (pts) of dimensionless duration $\mathscr{T}_{\mathtt{pts}} = 2t_1\omega_k$ (found using $Y_0 = -8R$, $U_{\mathtt{trans}} = 10\,\mathrm{m/s}$, $\omega_k = 0.5057\,\mathrm{rad/s}$) and trajectory directed towards the mid-span deck section ($X_0 = \ell_{\mathtt{cs}}/2$, $\ell_{\mathtt{cs}} = 3300\,\mathrm{m}$). Fig. 2(a) displays three consecutive repetitions. Fig. 2(b) demonstrates the asymmetry in the magnitude of the MS spatial intensification, which depends on $F_{\mathtt{fj}}(x)\mathrm{sgn}(X_0 - x)$ in Eq. (1) and the ratio $r_{UV} = U_{\mathtt{trans}}/V_{\mathtt{max}} = 0.12$ in this example. In Fig. 2(b) the main tornado core, centered around the deck cross-section ($X_0 = 1650\,m, y = 0$) and delimited by R, is represented by a dashed semicircular line.

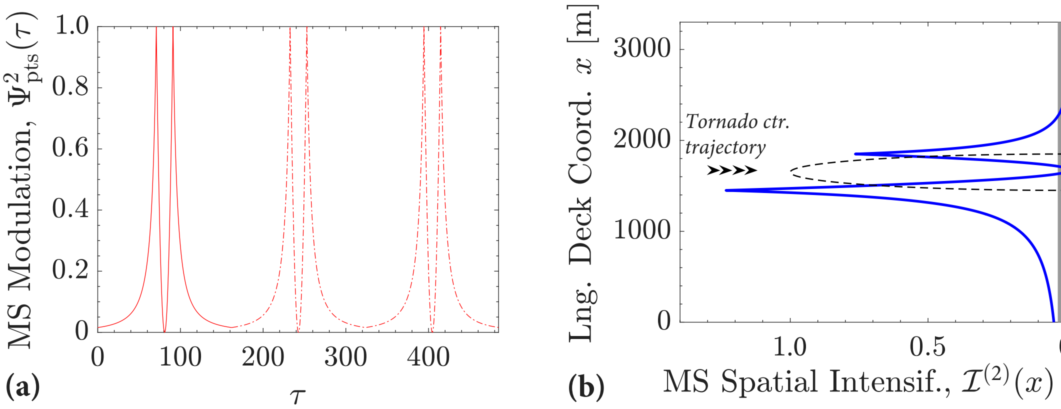

Figure 2. (a) Mean-square (MS) temporal modulation *vs.* τ, and (b) spatial intensification *vs.* longitudinal deck coordinate x of repeated Fujita tornadoes with radius $R = 200\,\mathrm{m}$ and trajectory towards mid-span ($X_0 = \ell_{\mathtt{cs}}/2$)

2.2. State-Space Dynamic Model

Although the standard flutter problem can be solved by multi-mode approach in the frequency domain [e.g., Jones and Scanlan (2001)], bridge flutter is examined in time domain (Caracoglia, 2025) since the formulation must consider non-stationary tornado outflow. The model is a two-mode approach, restricted to the coupling of the first vertical bending and torsional deck modes. Vertical and torsional degrees of freedom of each deck section respectively are: $h(x,\tau) \approx \xi_j(\tau)Bh_j(x)$, $\alpha(x,\tau) \approx \xi_k(\tau)\alpha_k(x)$; $h_j(x)$ and $\alpha_k(x)$ are dimensionless deck mode-shape functions of the purely vertical bending mode j and purely torsional mode k; and $\xi_j(\tau)$ and $\xi_k(\tau)$ are generalized coordinates with time $\tau = t\omega_k$. Coupled-mode flutter is examined after re-writing the equations as a first-order, state-space system with $\mathbf{z}_{\mathtt{AE}}(\tau)$ state vector of dimension $n_{\mathtt{AE}}$:

$$\mathrm{d}\mathbf{z}_{\mathtt{AE}}(\tau)/\mathrm{d}\tau = \mathbf{A}_{\mathtt{AE}}(\tau)\mathbf{z}_{\mathtt{AE}}(\tau) \tag{3}$$

The linear state matrix is $\mathbf{A}_{\mathtt{AE}}(\tau)$ is time-dependent and periodic because it depends on $\Psi_{\mathtt{pts}}^2(\tau)$ modulation with dimensionless period $\mathscr{T}_{\mathtt{pts}} = 2t_1\omega_k$; $\mathbf{A}_{\mathtt{AE}}(\tau)$ also depends on the intensity of the tangential, tornadic flow $V_{\mathtt{max}}$ and $\mathscr{I}^{(2)} > 0$ [Eq. (2)]. In Eq. (3), the effective angle of attack of the load ($\theta_{\mathtt{attack}}$ in Fig. 1) reverses at $x = X_0$, when finding the generalized loads by integration. As $V_{\mathtt{max}}$ increases to reach flutter condition, the elements of $\mathbf{A}_{\mathtt{AE}}(\tau)$ change.

3. PRELIMINARY RESULTS AND CONCLUSIONS

The Messina Bridge (1992 design) is modeled according to Diana et al. (1995). The deck width is $B = 62.0\,\mathrm{m}$; the central span length is $\ell_{\mathtt{cs}} = 3300\,\mathrm{m}$. The analysis uses the first two asymmetric deck modes, the first bending mode j (mode 3 of the bridge) and the first torsional mode k (mode 4 of the bridge with angular frequency $\omega_k = 0.506\,\mathrm{rad/s}$). The Scanlan derivatives measured by Zasso (1996) and supplementary data by Baldomir et al. (2013) are used to find the deck indicial functions (Caracoglia, 2025). The flutter-like tornado study considers the Fujita tornado described in the previous section (Fig. 2). The strike periodicity is $\mathscr{T}_{\mathtt{pts}} = 161.8$ (320 seconds). Fig. 3 illustrates results of a preliminary time domain simulation, considering the strike of three consecutive tornadoes at various $V_{\mathtt{max}}$. Diverging deck vibration (about 3°at $x = \{0.25, 0.75\}\ell_{\mathtt{cs}}$) is noted at $V_{\mathtt{max}} = 193\,\mathrm{m/s}$, compared to flutter speed under stationary, uniform wind field [88.5 m/s, Caracoglia (2025)]. More details will be presented at In-Vento.

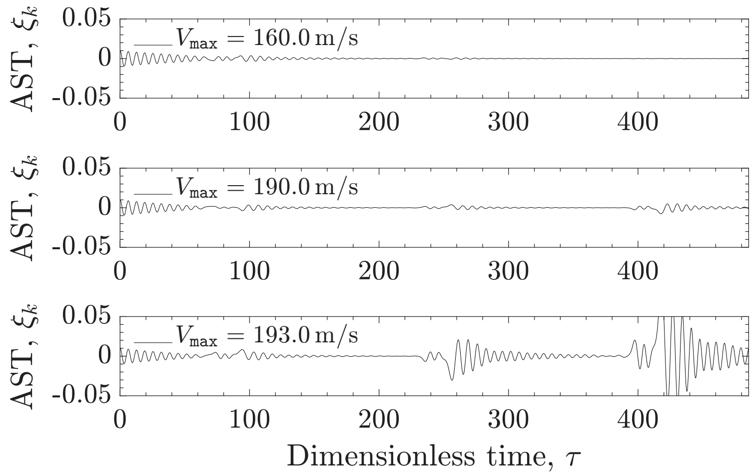

Figure 3. Tornado-like flutter analysis of the Messina Bridge model: generalized response ξ_k of the first a-symmetric (AST) torsional deck mode vs. time $\tau = t\omega_k$ at tangential speeds $V_{\mathtt{max}} = \{160, 190, 193\}$ m/s.

ACKNOWLEDGEMENTS

This work was supported in part by the National Science Foundation, Award CMMI-2330150, subcontracted from Iowa State University (USA); the research is led by Professor Partha P. Sarkar, who is gratefully acknowledged.

REFERENCES

Baldomir, A., I. Kusano, S. Hernandez, and J. Jurado (2013). A reliability study for the Messina Bridge with respect to flutter phenomena considering uncertainties in experimental and numerical data. Comput. Struct. 128, 91–100.

Cao, J., S. Ren, S. Cao, and Y. Ge (2019). Physical simulations on wind loading characteristics of streamlined bridge decks under tornado-like vortices. English. J. Wind Eng. Ind. Aerodyn. 189, 56–70.

Caracoglia, L. (2025). Long-span bridge flutter analysis in non-stationary downburst-like flows by Floquet Theory. J. Wind Eng. Ind. Aerodyn. 264, 106138.

Diana, G., M. Falco, S. Bruni, A. Cigada, G. Larose, A. Damsgaard, and A. Collina (1995). Comparisons between wind tunnel tests on a full aeroelastic model of the proposed bridge over Stretto di Messina and numerical results. J. Wind Eng. Ind. Aerodyn. 54-55, 101–113.

Fujita, T. (1978). *Workbook of Tornadoes and High Winds for Engineering Applications*. Tech. rep. U.S. Department of Energy - Division of Operational and Environmental Safety.

Jones, N. P. and R. H. Scanlan (2001). Theory and full-bridge modeling of wind response of cable-supported bridges. J. Bridge Eng.-ASCE 6, 365–375.

Scanlan, R. H., J. G. Béliveau, and K. S. Budlong (1974). Indicial aerodynamic functions for bridge decks. J. Eng. Mech.-ASCE 100, 657–673.

Zasso, A. (1996). Flutter derivatives: advantages of a new representation convention. J. Wind Eng. Ind. Aerodyn. 60, 35–47.